



Prussian Blue Nanowires Fabricated by Electrodeposition in Porous Anodic Aluminum Oxide

Haiqing Luo,^a Xingguo Chen,^{a,z} Pingheng Zhou,^b Huigang Shi,^b and Desheng Xue^b

^aDepartment of Chemistry and ^bKey Laboratory for Magnetism and Magnetic Materials of MOE, Lanzhou University, Lanzhou 730000, China

Highly ordered prussian blue (PB) nanowire arrays were fabricated successfully for the first time by self-assembling in a nanoporous anodic aluminum oxide template. The nanowires with different lengths and diameters could be obtained by controlling, respectively, the deposition time and the size of the nanohole in the template. The structure and morphology of the nanowires were characterized by X-ray diffraction, transmission electron microscopy, and selected area electron diffraction. The results showed each of the nanowires was a continuous and preferentially of single crystal with face-centered-cubic structure. The Curie temperature T_c of PB nanowires was lower with respect to that of PB bulk. The growth mechanism of the nanowire is also discussed. © 2004 The Electrochemical Society. [DOI: 10.1149/1.1775223] All rights reserved.

Manuscript submitted June 30, 2003; revised manuscript received January 26, 2004. Available electronically August 11, 2004.

Among the known molecular magnets, prussian blue (PB) (catena-[MFe^{II}Fe^{III}(CN)₆])(M = Li⁺, Na⁺, K⁺, NH₄⁺) and related cyano-metallate-based coordination polymers offer a range of compounds with unique versatility. The variety of structures and magnetic properties of this family of compounds have been extensively investigated,^{1,2} and recently reviewed.³⁻⁵ Although much work has focused on the relationship between the unit cell structure and magnetic properties, relatively few studies have been made on the growth mechanism, synthesis fashion, and method of controlling the growing process. These are important aspects in the study of molecular magnets, because compounds with appropriate magnetic properties can be acquired by controlling the shape of the magnets. Recently, different methods mainly in the solution-phase route have been used to fabricate types of PB such as powder, bulk, thin film, and nanoparticles.⁶⁻⁸ Moreover, many studies have also been focused on the preparation and electrochemical behavior of PB and its analogues.⁹⁻¹⁵ To our knowledge, no study except our prior work on the PB nanowire has been reported.¹⁶

Synthesis of nanowire arrays by means of electrodeposition into the porous anodic aluminum oxide (AAO) template is a popular method. In this method, the nanowire diameter can be determined by the size of the nanohole, which can be controlled by adjusting the oxidation voltage in types of anodizing solutions. As a result of nanosize effect, the nanowire arrays show different characteristics compared with bulk or other morphologic materials. However, most of the nanowire arrays prepared by the alternating current (ac) electrodeposition method are metal and alloys.

In this work, according to the electrodepositing fabrication of PB film by Neef,¹⁰ we first fabricated the PB nanowire arrays by the ac electrodeposition into the porous AAO template. The possible growth mechanism of the nanowire is discussed.

Experimental

Fabrication of AAO.—We have fabricated the AAO template by the following process according to the two-step electrochemical anodization.¹⁷⁻¹⁹ First, high purity (99.99%) aluminum foils were annealed at 600°C for 6 h. Subsequently, the sample was ultrasonically degreased in acetone, and cleaned in 5% NaOH at 15°C for 20 min, and a smooth surface was obtained. Then, the aluminum was electropolished in a 25:75 volume mixture of HClO₄ and C₂H₅OH. The polished Al samples were anodized at 40 V_{DC} in 2.7 wt % (0.3 M) H₂C₂O₄ at 10°C, which contained the following four steps: (i) anodized a polished Al sheet for 30 min; (ii) dissolved away the oxide film in a mixed solution of 0.2 M H₂CrO₄ and 0.4 M H₃PO₄ at 60°C for 5 min; (iii) rinsed the Al sheet with deionized water,

then anodized it for 1-3 h; (iv) removed the oxide film, and anodized the Al sheet for 1 h again. Consequently, a AAO template with highly ordered pore arrays was obtained.

Synthesis of the PB nanowire arrays.—Electrodeposition of the PB nanowires was carried out using a standard double-electrode cell. The work electrode (a porous alumina template) and the counter electrode (pretreated graphite) were submerged in a fresh solution of 0.02 M FeCl₃, 0.02 M K₃Fe(CN)₆, 0.6 M H₃BO₃, and 0.5 M KCl. The electrodeposition progress was kept for 3 min under 1 Hz 13 V_{AC}. After electrodeposition, the resulting oxide layer with nanowire arrays was removed in a saturated HgCl₂ solution from the remaining aluminum. Then the free-standing nanowires were obtained by dissolving away the aluminum oxide film in a mixed solution of 0.1 M H₂CrO₄ and 0.1 M H₃PO₄ at room temperature.

Instruments.—Surface morphology of the AAO template was studied using a JSM-5600LV scanning electron microscope (SEM), X-ray diffraction (XRD, Rigaku/Max-2400) with Cu K α ₁ radiation was used to identify the phase and analyze the structure of the PB nanowires. Transmission electron microscopy (TEM) and selected area electron diffraction (SEAD) were performed to probe the microstructure and morphology of the sample by using a JEO 2000 X microscope at an operating voltage of 75-100 kV. The magnetic properties of the PB nanowire arrays were investigated with the magnetic property measurement system (MPMS).

Results and Discussion

Figure 1a-b show the SEM micrographs of different AAO templates. The pore diameters of 55 and 290 nm were obtained in oxalic and phosphoric acid solutions under voltages of 40 and 150 V, respectively. The arrays with highly ordered pores are displayed in the alumina templates. The uniform pores can be seen in the AAO templates, especially the perfectly hexagonal ordered domains can be formed over a wide range of pore distances in the AAO template fabricated at 40 V in oxalic acid solution (Fig. 1a). It was reported that the pore diameter and distance were determined by anodic voltage and a variety of anodic acids.^{20,21} In this work, the results indicate that the AAO of different sizes range from several tens to hundreds of nanometers can be achieved by adjusting the height of the voltage in types of anodizing solution such as sulfuric, oxalic, and phosphoric acid.

Figure 2 shows the TEM image of the PB nanowires with the average length and diameter of 4 μ m and 55 nm, which was fabricated in the AAO template anodized at 40 V_{DC} in 0.3 M H₂C₂O₄. The results indicate that the diameter of the PB nanowires is consistent with that of the deposited AAO nanoholes. So the uniform length and diameter of nanowires can be prepared by controlling the depositing time and the pore diameter of the AAO template.

The XRD patterns of the PB nanowire arrays and the PB bulk are shown in Fig. 3. The results indicate the nanowire has a face-

^z E-mail: chenxg@lzu.edu.cn

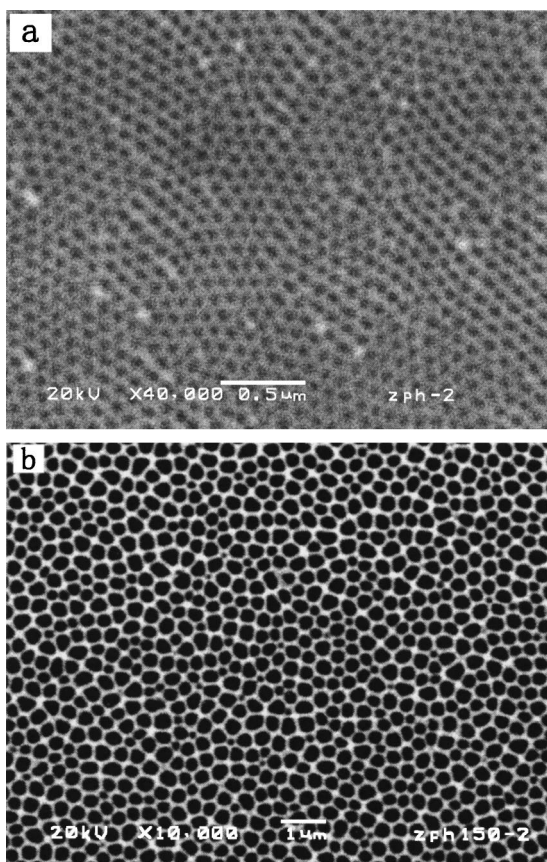


Figure 1. Micrographs of the bottom view of anodic alumina layers. Anodization was conducted in 2.7 wt % (0.3 M) oxalic acid at 10°C at 40 V (a), and 10 wt % phosphoric acid at 150 V (b). Pore opening was carried out in 5 wt % phosphoric acid at 20°C for 10 min.

centered-cubic (fcc) structure, which is similar to the PB bulk. The peak width of the nanowire arrays is noticeably larger than that of the bulk, which can be expected from the size effect of nanometer, the reason is not clearly known.

The SEAD pattern of a PB nanowire shown in Fig. 4a presents sharp diffraction spots, which can be indexed as (040), (440). Figure 4b is the dark-field TEM image of the same nanowire. Both indicate that the nanowire is dense, continuous, and tends to be single crystal. However, when the temperature goes up to 100°C, the crystal

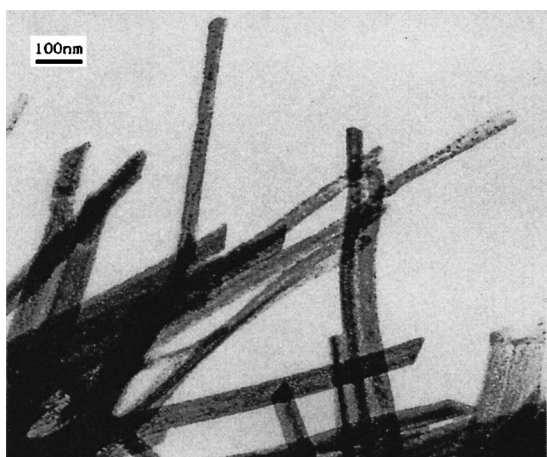


Figure 2. TEM morphology of the PB nanowires.

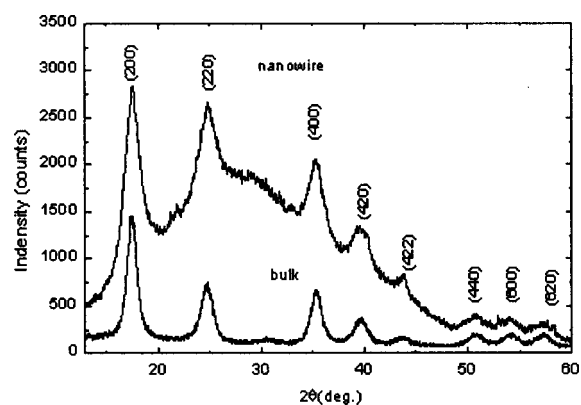


Figure 3. XRD patterns of PB bulk and alumina template filled with the PB nanowires, using Cu $K\alpha_1$ radiation.

nanowire may easily partially dehydrate by thermal decomposition. The single crystal turned into polycrystalline, and the SEAD pattern became diffraction rings, which can be seen in Fig. 4c. The diffraction rings can be indexed as (222), (400), and (440) reflections from fcc structure of PB.

The infrared spectrum measured at room temperature in the region from 2000 to 2200 cm^{-1} shows one peak at 2158 cm^{-1} , which is due to the stretching of CN in the $\text{Fe}^{\text{II}}\text{-CN-Fe}^{\text{III}}$ links. So the oxidation state of the iron ions in PB nanowire can be expressed as $\text{Fe}^{\text{II}}\text{-CN-Fe}^{\text{III}}$, similar to the PB bulk. The field-cooled magnetization vs. temperature of PB nanowires at $H = 10$ Gs shows a $T_c = 4.1$ K which is lower with respect to that of PB bulk, $T_c = 5.6$ K (Fig. 5). The susceptibility measurement were carried out from $T = 1.9$ to 10 K. The linear part of the χ_M^{-1} vs. temperature curve was fitted to the Curie-Weiss law $\chi_M = C/(T-\theta)$. It is concluded that the Weiss constant θ is 3.76 K, which indicates a long ferromagnetic interaction between the Fe^{3+} ions through the cyanide bridge and diamagnetic Fe^{2+} ions.

In the depositing solution, we selected H_3BO_3 as a buffer system. This may assure the stability of the depositing solution at the same time, the H_3BO_3 cannot dissolve the layer of alumina. As there is an Al_2O_3 barrier layer between the porous alumina film and metallic Al sheet, in order to make the barrier layer thinner, the voltage was decreased to 5-7 V by the speed of 2 V per 2 min after the end of the two-step anodization. Using only the treated AAO by this method, we can deposit PB nanowires. PB was dissolved quickly in alkalis such as the NaOH solution, and alumina was dissolved slowly in acids such as the H_2SO_4 or HCl solutions. Then we selected the mixture solution of phosphoric and chromic acids to obtain the preferable freestanding PB nanowires by dissolving away the aluminum oxide film.

In this work, to get the optimum condition for fabricating the best PB nanowires, a series of experiments with different electrodeposition conditions was performed. Also high quality deposition of the PB nanowires was obtained with ac frequency from 1 to 3 Hz and ac voltage from 12 to 13 V. When the frequency or voltage of the ac was higher than the upper boundary of the optimal range, there was little or no deposition. It may be seen clearly that H_2 emerges from AAO by giving an ac voltage higher than 15 V. We fabricated the PB nanowires with different lengths by controlling the electrodeposition time. However, if the deposition time was over 4 min, a thin film on the surface of AAO resulted.

Based on the fabrication of PB film by electrodeposition and the results of the experiment, the possible primary growth mechanism of the PB nanowires is discussed as follows. Figure 6 shows the device of a double electrode system for electrodeposition. During the processing of electrodeposition, the electrons come to the bottom of the nanohole of AAO by tunnelling the thin barrier layer, and

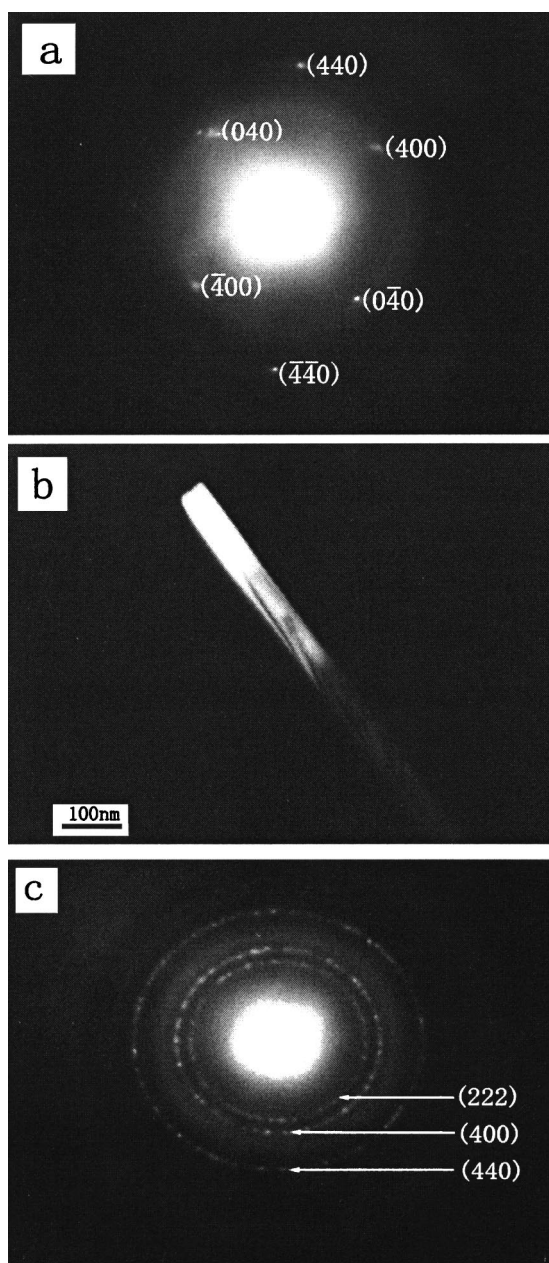
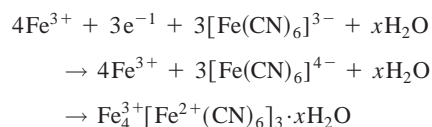


Figure 4. (a) Electron diffraction patterns for a single PB nanowire. (b) Dark-field image of a single PB nanowire. (c) Electron diffraction patterns for a dewatered PB nanowire.

$[\text{Fe}(\text{CN})_6]^{3-}$ was reduced to $[\text{Fe}(\text{CN})_6]^{4-}$ while capturing an electron. Then $[\text{Fe}(\text{CN})_6]^{4-}$ combined with Fe^{3+} in the solution. Subsequently the PB molecule is deposited at the bottom of nanoholes. The electrochemical reaction can be formulated as¹⁶



By the constant tunnelling of electrons, the PB nanowire comes into being by deposition outwards from the nanohole.

Generally, each of the metal and alloy nanowires prepared by ac electrodeposition method in AAO is composed of particles of crystals, while the PB nanowire fabricated in this work is a dense, continuous, and preferable crystal resulting from the SEAD and TEM.¹⁶

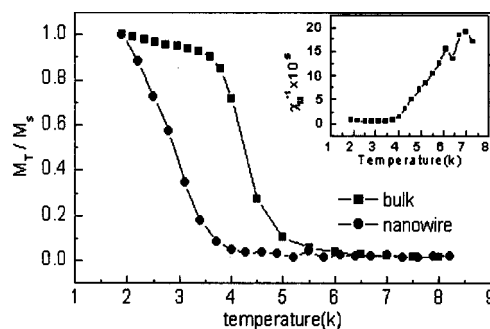


Figure 5. Field-cooled magnetization vs. temperature curves at $H = 10$ Gs, thermal variation of the susceptibility of the PB nanowire, χ_M^T vs. T (insert).

This may result from the different properties of the metal and PB in the nature of the PB. The metal or alloy is composed of atoms combined by a metal bond, and the atom can lose its free electrons in the outer electron shell easily. However, it needs a certain energy to overcome the electrostatic attractive forces when the atoms of the metal and alloy enter solution from the solid phase by losing electrons. During the progress of electrodeposition, an ac of the sine signal was used. Therefore the electrodeposition of metal or alloy nanowire is a nonequilibrium process combining deposition and dissolution. In a practical sense, the tendency of the deposition speed for metal and alloy is a little larger than that of the dissolution speed, which results in some remainders in the nanohole. Then the remainders accumulate constantly and grow into a polycrystalline nanowire. However, the growing process of the PB nanowire is different. First, as soon as $[\text{Fe}(\text{CN})_6]^{3-}$ was reduced to $[\text{Fe}(\text{CN})_6]^{4-}$, the latter combined with Fe^{3+} immediately and formed a PB precipitate ($\text{Fe}_4^{3+}[\text{Fe}^{2+}(\text{CN})_6]_3 \cdot x\text{H}_2\text{O}$) in the nanoholes. On the other hand, the PB has a steady structure of fcc, Fe^{2+} present in $\text{Fe}_4^{3+}[\text{Fe}^{2+}(\text{CN})_6]_3$ is held to CN^- tightly by a coordination bond. So it is very difficult for Fe^{2+} among the PB framework to reenter the solution by losing an electron. That is, the growth of the PB nanowire is mainly a continuous deposition process with little dissolution, which results in the preferable formation of a single-crystal nanowire outwards from the nanohole of AAO.

Conclusions

First we have fabricated PB nanowire arrays successfully by ac electrodeposition into the nanoporous AAO template. The TEM and SEAD results show that the nanowire is a dense, continuous, and preferentially single crystal with a structure of fcc. By controlling the conditions of the fabrication of AAO and the time of electrodeposition, the nanowires with uniform diameter and length were obtained by self-assembly. Magnetic measurement results indicate that the Curie temperature of the PB nanowire decreases as the average number of magnetic interaction neighbors is reduced. It may

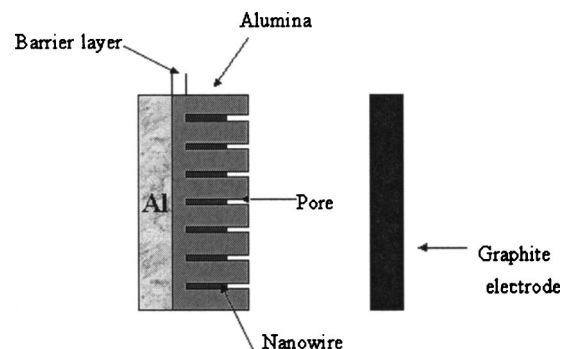


Figure 6. Device of double-electrode system for electrodeposition.

be a new approach to fabricate nanowires of some coordination complex. Compared with PB bulk or other morphologies, it is expected that the PB nanowire has many different and unique advantages in magnetic, electric, and optical properties *et al.* Various further studies are in progress.

Acknowledgments

This work was supported by National Natural Science Foundation (grant no. A10174027) and EYTP of China. X.C. thanks the Visiting Scholar Foundation of Key Lab for Magnetism and Magnetic Material of MOE.

References

1. S. Ferlay, T. Mallah, R. Ouahés, P. Veillet, and M. Verdager, *Nature (London)*, **378**, 701 (1995).
2. S. Ohkoshi, Y. Abe, A. Fujishima, and K. Hashimoto, *Phys. Rev. Lett.*, **82**, 1285 (1999).
3. C. T. Kresge, M. E. Leonowicz, W. E. Roth, J. C. Vartuli, and J. S. Beck, *Nature (London)*, **359**, 710 (1992).
4. S. Mann, S. L. Burkett, S. A. Davis, C. E. Fowler, N. H. Mendelson, S. D. Sims, D. Walsh, and N. T. Whilton, *Chem. Mater.*, **9**, 2300 (1998).
5. C. G. Göltner, S. Henke, M. C. Weisenberger, and M. Antonietti, *Angew. Chem., Int. Ed. Engl.*, **37**, 613 (1998).
6. B. R. E. Wilde, S. N. Ghosh, and B. J. Marshall, *Inorg. Chem.*, **9**, 2512 (1970).
7. Y. Z. Guo, A. R. Guadalupe, O. Resto, L. F. Fonceca, and S. Z. Welsz, *Chem. Mater.*, **11**, 135 (1999).
8. S. Vaucher, M. Li, and S. Mann, *Angew. Chem., Int. Ed. Engl.*, **39**, 1793 (2000).
9. P. J. Kulesza, *J. Electroanal. Chem.*, **289**, 103 (1990).
10. V. D. Neef, *J. Electrochem. Soc.*, **125**, 886 (1978).
11. C. A. Lundgren and R. W. Murray, *Inorg. Chem.*, **27**, 933 (1988).
12. H. Masui and R. W. Murray, *J. Electrochem. Soc.*, **145**, 3788 (1998).
13. K. Itaya, I. Uchida, and V. D. Neff, *Acc. Chem. Res.*, **19**, 162 (1986).
14. A. Dostal, B. Meyer, F. Scholz, U. Scheroder, A. M. Bond, F. Marken, and S. J. Shaw, *J. Phys. Chem.*, **99**, 2096 (1995).
15. P. J. Kulesza, S. Zamponi, M. Berrettoni, R. Marassi, and M. A. Malik, *Electrochim. Acta*, **40**, 681 (1995).
16. P. H. Zhou, D. S. Xue, H. Q. Luo, and X. G. Chen, *Nano Lett.*, **2**, 845 (2002).
17. H. Masuda and K. Fukuda, *Science*, **268**, 1466 (1995).
18. H. Masuda, F. Hasegawa, and S. Ono, *J. Electrochem. Soc.*, **144**, L127 (1997).
19. F. Y. Li, L. Zhang, and R. M. Metzger, *Chem. Mater.*, **10**, 2473 (1998).
20. K. Ebihara, H. Takahashi, and M. Nagayama, *J. Met. Finish. Soc. Jpn.*, **34**, 548 (1993).
21. A. P. Li, F. Müller, A. Birner, K. Nielsh, and U. Gösele, *J. Appl. Phys.*, **84**, 6023 (1998).